RESEARCH ARTICLE

Simultaneous Measurement of Patellofemoral Joint Kinematics and Contact Mechanics in Intact Knees: A Cadaveric Study

Wenhan Huang, PhD[1,2#], Xiaolong Zeng, PhD[1#], Gene Chi-Wai Man, PhD[2], Liu Yang, PhD[2,3], Yu Zhang, PhD[1]

[1]*Department of Orthopaedics, Guangdong Provincial People's Hospital, Guangdong Academy of Medical Sciences, Guangzhou and* [3]*Department of Bone and Joint Surgery, Shenzhen People's Hospital, Shenzhen, China and* [2]*Department of Orthopaedics & Traumatology, Faculty of Medicine, Shatin, Hong Kong*

Objective: Patellofemoral kinematics and contact mechanics are important measurements for the assessment of patellofemoral joint (PFJ) problems. Simultaneously measuring PFJ contact pressures and kinematics is a challenging task. The purpose of this study was to simultaneously measure the kinematics and mean/peak contact pressures in the PFJs of cadaveric knees.

Methods: This was a comparative study performed on fresh cadaveric knees. The kinematic data was acquired for nine cadaveric knees using an optical tracking system. Data about the contact pressure and contact area in the PFJ was obtained at knee flexion angles of 0°, 30°, 60°, 90°, and 120° using a pressure sensor. Intraclass correlation coefficients (ICCs) and minimal detectable differences (MDDs) of six degrees of freedom (6 DOF) in the PFJs were calculated. ICCs and the MDDs of contact pressure, peak pressure, and contact area in the PFJs were also analyzed. We also compared the kinematics of the cadaveric knees before and after the insertion of the pressure sensor.

Results: All ICC values of 6 DOF in the PFJs were found to be greater than or equal to 0.924. Regarding medial–lateral rotation, the patellar showed a simplified movement pattern that demonstrated progressive lateral rotation of $4.8° \pm 3.4°$ at 120° of knee flexion. While for patellar tilting, the patella showed medial tilting that peaked at $7.2 \pm 2.5°$ at 30° of knee flexion. Whereas no significant differences in PFJ kinematics were found between with and without the placement of the pressure sensor at all knee flexions ($P > 0.05$). Most of the ICC values for contact pressure, peak contact pressure, and contact area ranged from 0.8 to 0.9. The MDDs for rotational displacement were 0.9° and 0.6 mm for translational displacement. No statistical differences in patellar kinematics were found before and after the insertion of the pressure sensor.

Conclusions: The setup in the present study enables researchers to simultaneously and synchronously collect real-time PFJ kinematics and tibiofemoral joint (TFJ) biomechanical kinematic data with high reliability. The low MDDs enabled the researchers to obtain an accurate interpretation of the kinematic and contact mechanics measurement using the experimental setting used in the present study.

Key words: Biomechanics; Cadaver; Kinematics; Knees; Osteoarthritis; Patellofemoral Joint

Introduction

Patellofemoral kinematics and contact mechanics are important measurements for the assessment of patellofemoral joint (PFJ) problems, including anterior knee pain, patella dislocation, and PFJ osteoarthritis (OA). The relationship between the patella and the femur should be accurately defined to improve the general understanding of the etiology and mechanism of PFJ pathology. From a

Address for correspondence Wenhan Huang, Department of Orthopedics, Guangdong Provincial People's Hospital, Guangdong Academy of Medical Sciences, Room 1042, 10/F, Main Clinical Building, Zhongshan 2 Road, Guangzhou, 510317, Guangdong, China. Email: wenhanx@126.com
[#]These authors contributed equally to this work.
Received 27 November 2020; accepted 13 June 2022

biomechanical point of view, the PFJ acts as a lever that transmits the force of the quadriceps muscle to the lower leg *via* the patellar tendon. The PFJ kinematics describe the relative motion between the patella and the femur in the PFJ, including patella medial/lateral rotation, tilting and translation. The PFJ kinematics, also refer to patellar tracking, have influences on the pattern of contact area during knee flexion, and therefore dynamically affect the contact force distribution in the PFJ.[1]

Simultaneous measurement of PFJ kinematics and biomechanics enable the researchers to investigate the relation between the kinematic alterations and contact mechanics in an instantaneous manner. Therefore, it is very important to simultaneously and synchronously collect real-time PFJ kinematic and biomechanical data. Doing so can be very beneficial to investigations into the relationships between different variables of the PFJ. In previous studies, researchers have used customized loading apparatus to investigate patellar kinematics. Although the investigation techniques used in these studies were demonstrated to have validity and efficacy based on their protocols, quadriceps muscle loading and loading directions are not physiologically-based. Hence, they cannot accurately simulate *in vivo* conditions.

Varying quadriceps and hamstring muscle loadings ranging from 10 to 350 N have been used in different experimental settings.[2–5] These variations lead to inconsistencies in kinematic results. For example, Koh *et al.* found an increase in lateral tilt with increasing knee flexion,[6] whereas Brossmann *et al.* found the opposite.[7] In addition, the measurements of *in vitro* kinematics and contact pressure and distribution in PFJ in previous studies were not conducted simultaneously, so they were unable to show the relationship between PFJ kinematics and contact mechanics. In the current study, we used an optical tracking system to measure PFJ kinematics *in vitro* simultaneously with physiological quadriceps loading and loading direction data.

Increased contact pressure is considered to be one of the main factors that lead to the degeneration of articular joints. Therefore, it is critical to measure alterations in contact pressure in cadaveric human knees. In previous studies, sensitive films were inserted onto the surface of the patella for measurement.[8,9] However, the sensor films were inserted through lateral parapatellar incisions, and it is believed that PFJ biomechanics can be greatly affected by such incisions.[10,11] In the study by Haver *et al.*, contact sensors were used to measure contact pressure because of their high accuracy and analyzability.[10,12,13] As reported in previous studies, an identical incision was used for the placement of the contact sensors, and the researchers argued that the soft tissue surrounding the patella is kept intact using this approach.[3,14,15] It is believed that keeping the structures around the patella intact is a key factor in PFJ biomechanical evaluations because these structures play important roles in PFJ biomechanics. Once positioned to cover the patellar and trochlear surfaces, the film was secured to the local soft tissue with sutures at either of the distal corners to prevent it from moving within the joint cavity during knee extension. However, the test–retest reliability of this protocol and the MMDs for the contact mechanics measurement in the PFJ remain largely unknown, limiting the interpretability of this popular measure.

Therefore, the aim of this study was to validate the accuracy and reproducibility of PFJ kinematics and simultaneous contact mechanics measurement *via* an incision between the patella and trochlea. We hypothesized that no statistical differences in patellar kinematics would be found before and after the insertion of the pressure sensor.

Methods

Specimens

Nine fresh-frozen cadaveric knee specimens (five male, four female) with a mean age 56 years (range 49–69 years) and no history of knee surgery or disease were used in the current study. The sulcus angle range of the included knee specimen was 128°–155°, the Insall–Salvati ratios ranged from 0.88–1.18, and both parameters were within the normal range for knees. Each specimen included the femur, tibia, and fibula, along with all associated tendons, muscles, fasciae, and ligaments. Each specimen was thawed for 24 hours at room temperature prior to testing and was regularly hydrated with normal saline. None of the subjects had been physically injured, and none of the specimens showed signs of advanced degeneration after arthroscopic knee inspection and X-ray scan. The authors had scanned the specimens with X-ray to exclude severe osteoarthritis and osteoporosis. The results indicated that no significant degeneration was found in the included knee specimens. This study was approved by the Institutional Review Board of Guangdong Provincial People's Hospital (No. 2020bq10). All procedures performed in this study were done so in accordance with the Declaration of Helsinki and its later amendments or comparable ethical standards. An illustrative workflow diagram is shown as Fig. 1.

Specimen Preparation

The knees were carefully dissected, leaving the PFJ, TFJ, periarticular skin, subcutaneous tissue, and the knee capsule intact. The quadriceps muscle and quadriceps tendon were left intact for clamping. The femur, tibia, and fibula were cut 25 cm from the tibial plateau. Care was taken to not violate the cartilaginous structures.

Experimental Setup

Motion Units and Range

The setup for this experiment consisted of a femur/tibia/patella unit. The femur was fixed onto a rigid cylindrical support using four screws through the bone to prevent movement. The TFJ was free and unconstrained, so the setup enabled full movement in the knee joint from full extension to 120° of knee flexion.

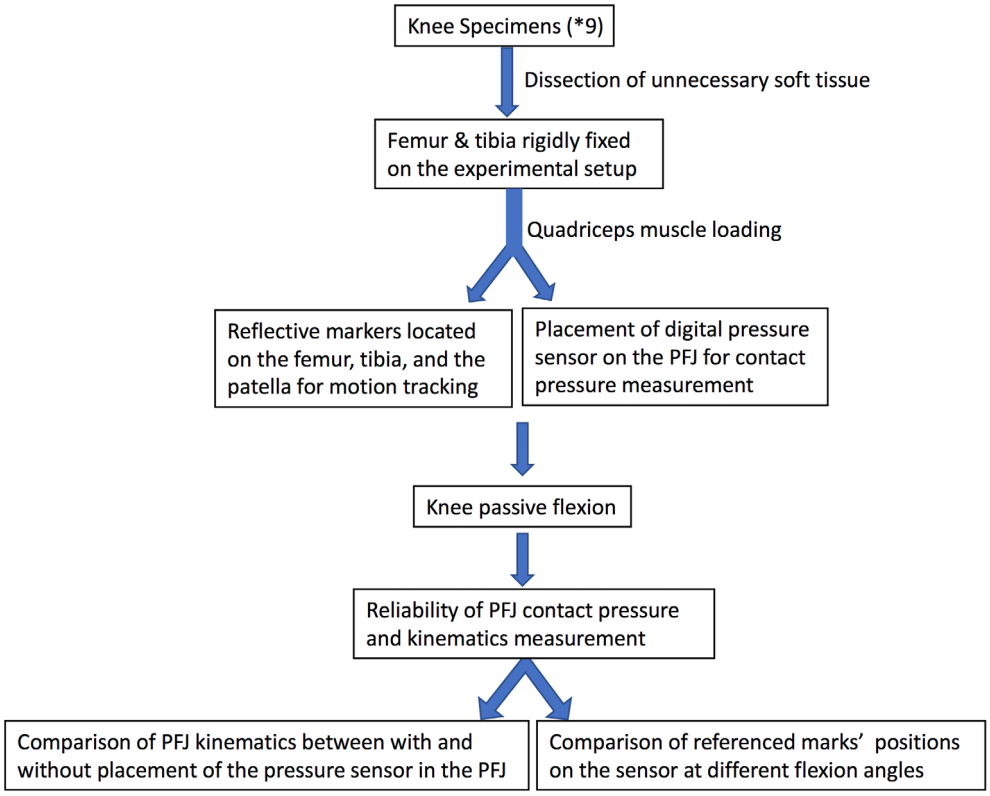

Fig. 1 Illustrative workflow diagram of this study. (PFJ: Patellofemoral Joint)

Muscle Loading and Directions

The quadriceps tendon was physiologically loaded with a 175-newton load using hanging weights. The knees were mounted onto the jig and the steel plates and pulleys were adjusted to match the orientation reported by Farahmand *et al.*[16] The muscles pulled in physiological directions relative to the axis of the femur: 20° lateral for VL, 5° anterior for RF + VI, and 35° medial for VM. A 175 N load was applied to the quadriceps; each muscle component was loaded by a cable to a percentage of the 175 N in proportion to its physiological cross-sectional area. The proportion of each muscle component was specified as below: 35% for VL, 40% for RF + VI, and 25% for VM.[5,17,18] The reason why we chose 175 N was based on the findings from the study by Shalhoub *et al.*[19] The 175 N weight used to load the quadriceps was chosen to avoid muscle rupture at the cable attachment and the researchers found that it was an upper limit in which there was no tearing of the muscle or failure of the suture site. This was done according to the directions and cross-sectional areas of the muscles.[20]

Motion Tracking Setting

To simplify the knee model, we did not use hamstring muscle loading because we used manual loading at the distal end of the tibia to act as hamstring muscle loading. This approach enabled us to observe the PFJ without the need to think about hamstring muscle loading because the PFJ biomechanical environment is isolated from the hamstring and related to quadriceps muscle loading. All three bone segments were identified *via* an optical rigid body equipped with bone pin markers so that relative movements of the three segments could be monitored, along with the six degrees of freedom (Fig. 2A, see Appendix S1 for more details).

Outcome Measurements

PFJ Kinematics

Coordinate System of the PFJ.. The coordinate system of the PFJ was built up to describe the patellar motions related to the femur (Fig. 2B). The femoral origin was located at the midpoint of the transepicondylar axis, a line connecting the prominent points of the medial and lateral femoral epi-condyles. The medial-lateral axis followed the transepicondylar line, the anterior–posterior axis was perpendicular to the plane defined by the transepicondylar line and the midpoint of the medial and lateral femur shaft, and the proximal-distal axis was set to be perpendicular to the other two axes. The midpoint of the line connecting the most medial and lateral points of the tibial plateau was defined as the origin of the tibial coordinate system. The medial-lateral axis followed the medial and lateral tibial plateau line, the anterior–posterior axis was perpendicular to the plane defined by the medial-lateral axis and the midpoint of medial and lateral tibia shaft, and the proximal-distal axis was set to be perpendicular to the other two axes. The midpoint of the line connecting the

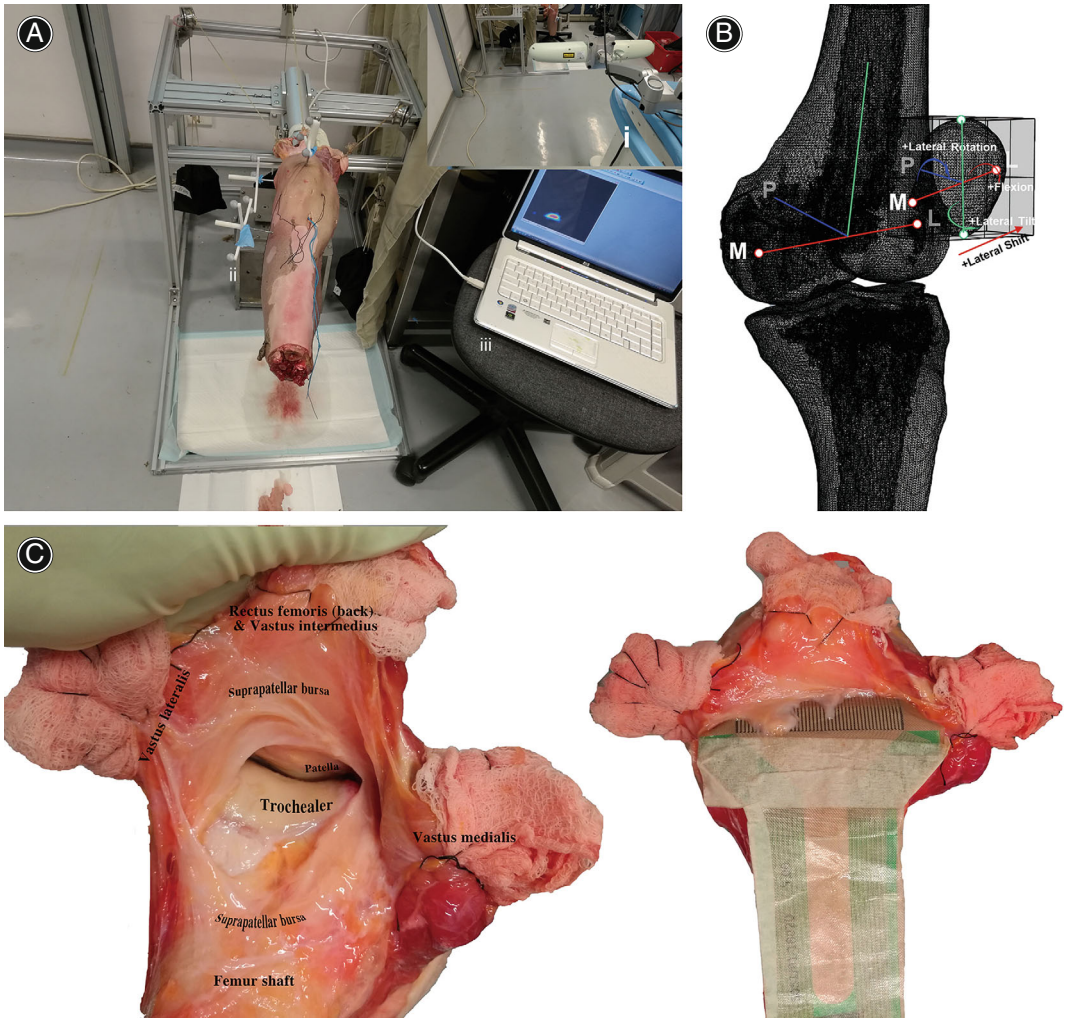

Fig. 2 Experimental setup of patellofemoral joint kinematics and biomechanics measurement. (A) i, Optiknee optical tracking system; ii, reflective markers; iii, TekScan system. (B) Established coordinate system for the patellofemoral joint and TFJ kinematics (Defined positive direction: lateral patellar tilt; external patellar rotation; patellar flexion; lateral patellar translation; posterior patellar translation; distal patellar translation). (C) Superior incision for the sensor placement beneath the patellofemoral pouch & quadriceps and anterior to the trochlea

most medial and lateral points of the patella was defined as the origin of the patella coordinate system. The medial-lateral axis followed the medial and lateral tibial plateau line, the anterior–posterior axis was perpendicular to the plane defined by the medial-lateral axis and the most proximal point of the patella, and the proximal-distal axis was set to be perpendicular to the other two axes.

PFJ Kinematics (Six Degree of Freedom of the PFJ)

We used six degrees of freedom of the PFJ which represented the PFJ kinematics to describe the relative movement between the patella and the femur. Specifically, the PFJ kinematics were divided into six freedoms:

1. Patellar tilting: patellar tilting was defined as the angle between the femoral and patellar axes in the axial plane.
2. Patellar flexion: patellar flexion angle was defined as the angle between the femoral and patellar axes in the sagittal plane.
3. Patellar rotation: patellar rotation was defined as the angle between the femoral and patellar axes in the coronal plane.
4. Patellar anteroposterior translations: it was defined as the shift between the origin of the femoral coordinate system and the origin of the patellar coordinate system in the sagittal plane.
5. Patellar mediolateral translations: it was defined as the shift between the origin of the femoral coordinate system and the origin of the patellar coordinate system in the coronal plane.
6. Patellar proximal-distal translations: it was defined as the shift between the origin of the femoral coordinate system

and the origin of the patellar coordinate system in the axial plane.

PFJ Contact Pressure and Areas

PFJ Contact Pressure

Mean contact pressure is the averaged pressure on the loaded sensels, which is calculated by dividing the force by the contact area. The "contact" values include only those sensels that have some (greater than zero) load applied to them. Peak contact pressureis the highest-pressure area in the object, calculated as the force inside the peak box divided by the peak box area; The "contact" values include only those sensels that have some (greater than zero) load applied to them.

PFJ Contact Area

Area of only the loaded, or 'contact' sensels include only those sensels that have some (greater than zero) load applied to them.

PFJ Kinematics Acquisition

The measurement space for this study was approximately 4.0 × 2.0 × 2.5 m^3 (Fig. 2A). The three-dimensional (3D) trajectories of the rigid bodies during knee motions were tracked using an integrated 2-headed stereo-infrared camera (NDI Polaris Spectra, Northern Digital Inc., Waterloo, Ontario, Canada) at a frequency of 60 Hz. In these three bone segments, there were three, six, and four bony landmarks respectively identified as bony landmarks to define the coordinate system established by Grood and Suntay and conduct data collection calibration.[21] A pin was inserted on the medial side of the femur 15 cm proximal to the joint line, and a second pin was positioned on the medial side of the tibia with the rigid body positioned in the sagittal plane 15 cm distal to the joint line. Then a third pin was inserted in the patella with the rigid body positioned in the sagittal plane. A handheld digitizing probe composed of four infrared light-reflecting markers was also used to identify femoral, tibial, and patellar landmarks. The landmarks included the midpoint of the medial and lateral femur shaft, lateral epicondyle, medial epicondyle, lateral plateau, medial plateau, tibial tuberosity, fibular head, the midpoint of the medial and lateral tibia shaft, proximal patella, distal patella, medial patella, and lateral patella.

The handheld probe was used to identify bone landmarks in a neutral position with the knee extended. This static position was used to establish the initial anatomical frame of reference to build up the joint coordinate system defined by Grood and Suntay (Fig. 2B). We set the value of all degrees of freedom to 0 in the initial position to make the results interpretable and comparable. First, we measured the PFJ kinematics when the pressure sensor was inserted into the PFJ. Second, we removed the pressure sensor and measured the PFJ kinematics again to investigate whether the placement of the pressure sensor affected the measurement of the PFJ kinematics.

PFJ Contact Areas and Pressure Acquisition

The PFJ contact pressure and contact area were simultaneously measured during knee flexion using an I-Scan 5051 pressure sensor (I-Scan, TekScan, Boston, MA, USA; Figure 2C). The sensor had a saturation pressure of 3.4 MPa, was 55.9 × 55.9 mm by 0.1 mm thick, and had 1936 pressure measurement points. To define the medial and lateral facets of the patella for our assessments of area and pressure distribution, a straight line connecting the superior and inferior points on the patellar ridge was drawn on the generated contact contours. After equilibration and calibration, the sensor was inserted through a superior incision in the patellofemoral pouch beneath the quadriceps and anterior to the trochlea. Once positioned to cover the patellar, it was secured in place with sutures in the local soft tissue at either of the distal corners to prevent it from moving in the joint cavity during knee extension. The sutures were positioned distal to the medial and lateral retinacula (Figure 2C). The measured PFJ kinematics were patellar medial-lateral rotation (degree), medial-lateral tilting (degree), and medial-lateral shift (mm) relative to femur.

Testing Procedure

To observe whether there was relative movement between the sensor and the patella that would affect the accuracy of measurement, we drilled two holes (3 mm in diameter) on the patella on the medial and lateral patellar sides in an anteroposterior direction (Fig. 3A). When we flexed the knee to 0°, 30°, 60°, 90°, and 120° of knee flexion, a pin was inserted into each hole in the patella to create reference marks on the sensor relative to the patella (Fig. 3B,C). We recorded the positions of the reference marks at every flexion angle mentioned above and compared the positions (Fig. 3D). If there was any relative movement generated during knee flexion, then the positions of the reference marks were different from each other, and *vice versa*.

Each specimen was tested three times and were conducted from knee extension (i.e., 0° of knee flexion) to 120° of knee flexion. The mean contact pressure, peak contact pressure, and contact area in the medial and lateral patellar facet during knee flexion were measured and analyzed.

Statistical Analysis

Data was analyzed with SPSS version 18 (IBM Corp, Armonk, NY, USA). The intra-rater reliability of the optical tracking system, contact pressure, peak contact pressure, and contact area were assessed using ICCs using a one-way random model. Specifically, regarding the intra-rater ICCs, ICC value measured at different flexion angles and the overall ICC value for every degree of freedom were calculated. Fleiss suggested that an ICC coefficient of >0.75 can be considered as evidence of good agreement between different ratings given by the same raters.[22] Moreover, in the present study,

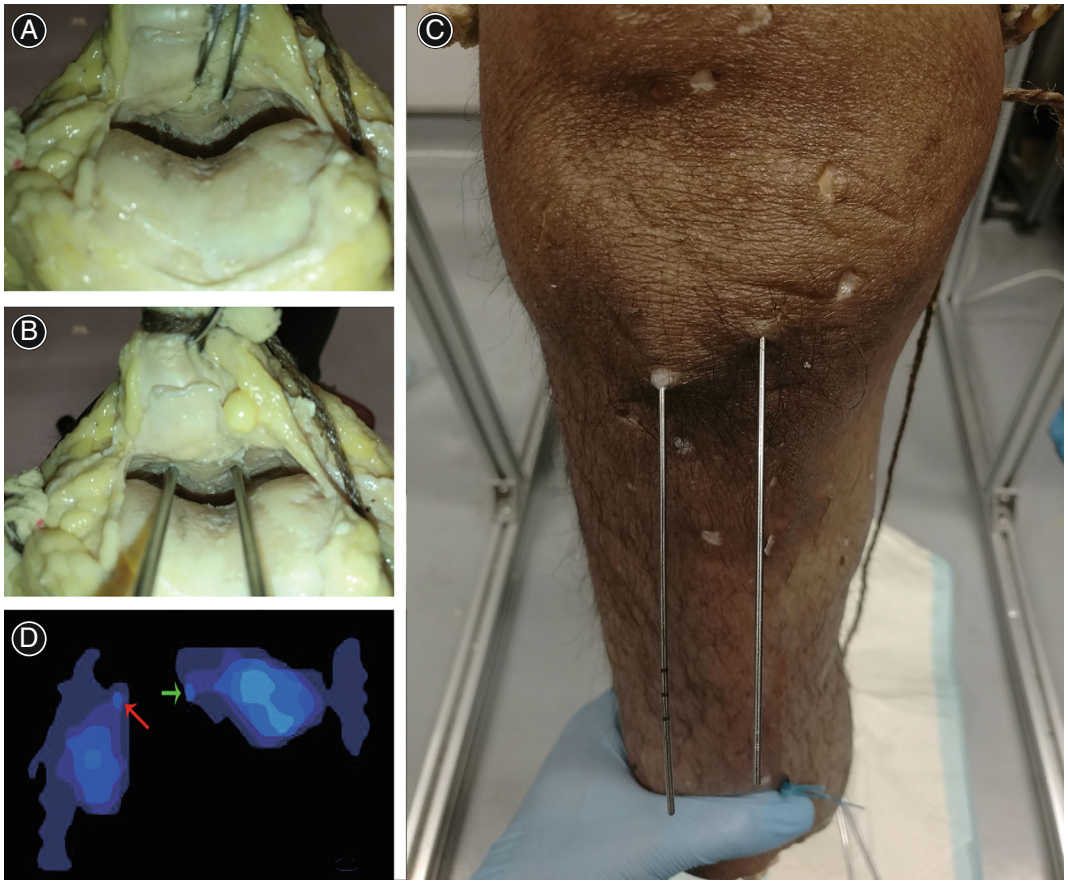

Fig. 3 Placement and validation of the pressure sensor. (A) Overview of the patellofemoral joint space prepared for the pressure sensor. (B) Two holes on medial and lateral sides of the patella in an anteroposterior direction. (C) Reference marks created on the sensor by pins inserted into each hole in the medial and lateral sides of the patella. (D) Front view of pins inserted into each hole in the medial and lateral sides of the patella

we defined that an ICC coefficient of >0.90 was required to achieve excellent reliability.

The minimum detectable differences (MDDs) of the six DOF and contact parameters were calculated based on the standard error of measurement (SEM) using the following formula:

$$\mathrm{MDDs} = 1.96 \,\mathrm{X}\, \sqrt{2}\, \mathrm{X}\, \mathrm{SEM}, \quad (1)$$

$$\mathrm{SEM} = \mathrm{SD}_{\text{all testing variables}}\, \mathrm{X}\, \sqrt{(1-\mathrm{r})}. \quad (2)$$

The $\sqrt{2}$ was used to account for the underlying added uncertainty during measurement at two time points. The value of 1.96 is the z score associated with the 95% confidence level, and r is the coefficient of the teste–retest reliability, which was estimated using an ICC. In addition, paired t-tests were conducted to compare the kinematics before and after the insertion of the pressure sensor at the flexion angles mentioned above. The significance level was set to 0.05.

A two-way repeated ANOVA measurement was performed to analyze the difference of contact pressure and contact area detected in medial and lateral patellar facet during knee flexion at 0°, 30°, 60°, 90°, and 120°. The primary factors are flexion angles and compartments (medial and lateral).

Results

PFJ Kinematics

PFJ Kinematics during Knee Flexion

The typical PFJ kinematic graphs for Knee 6 are shown in Fig. 4A. The results of three repeated trials are displayed, and they indicate that the testing protocol has high repeatability. The averaged patellar kinematics of the nine knees are shown in Fig. 4B. Regarding medial–lateral rotation, the patellar showed a simplified movement pattern, demonstrating progressive lateral rotation up to 4.8° ± 3.4° at 120° of knee flexion. For patellar tilting, during knee flexion, the patella showed medial tilting and peaked at 7.2° ± 2.5° at 30° of knee flexion. After that, it tilted reversely until it reached the end of flexion, but it maintained medial tilt

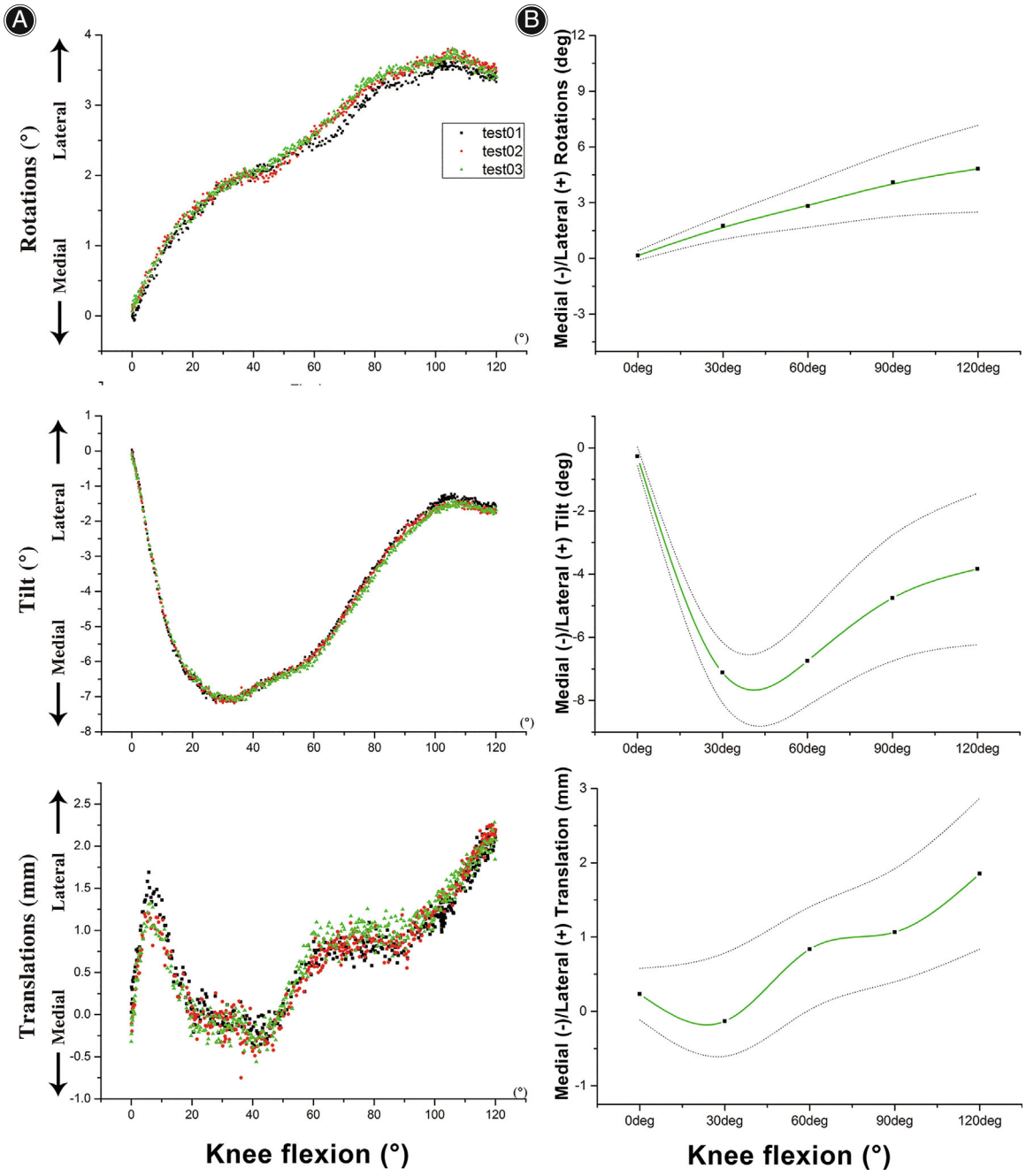

Fig. 4 Patellofemoral joint kinematics during knee flexion. (A) Representative illustration of patellar tilt, patellar rotations, and medial-lateral translation during knee flexion in intact knees. (B) Patellar tilt, patellar rotations, and medial-lateral translation in intact cadaveric knees

during the whole procedure. For translation, in general, the patellar showed a simplified movement pattern along the medial-lateral axis during knee flexion. The patella shifted increasingly laterally and peaked at around 1.7 ± 1.1 mm at 120° of knee flexion.

For the averaged changes of the PFJ kinematics during knee flexion in all testing knees, regarding internal-external rotation, the patella in ACL-intact knees showed a simplified movement pattern which demonstrating progressively lateral rotation up to 4.8° ± 2.3° at 120° of knee flexion. For patellar tilting, the patella showed medial tilting that peaked (7.1° ± 0.9°) at 30° of knee flexion. As the patella would tilted reversely till the end of flexion, it would maintain medial tilting during the whole procedure. For translation, in general, the patella showed fluctuating moving pattern along the medial-lateral axis during knee flexion. At the early phase

TABLE 1 Intra-rater reliability (intra-class correlation) of six degrees of freedom in the PFJ

ICCs	At specific flexion angles					Overall	MDDs[a]
	0°	30°	60°	90°	120°		
Rotation	0.998	0.989	0.924	0.997	1	0.988	0.35
Tilting	0.999	1	0.955	0.998	0.998	0.993	0.20
Flexion	1	1	1	0.999	1	0.999	0.91
AP	1	0.979	1	0.999	0.999	0.997	0.25
PD	1	0.998	1	1	1	0.999	0.04
ML	0.999	0.988	0.992	0.980	0.963	0.985	0.6

Abbreviations: AP, anterior–posterior translation; MDDs, Minimal detectable changes; ML, medial-lateral translation; PD, proximal-distal translation.; [a]The unit is degree for rotations and mm for translations.

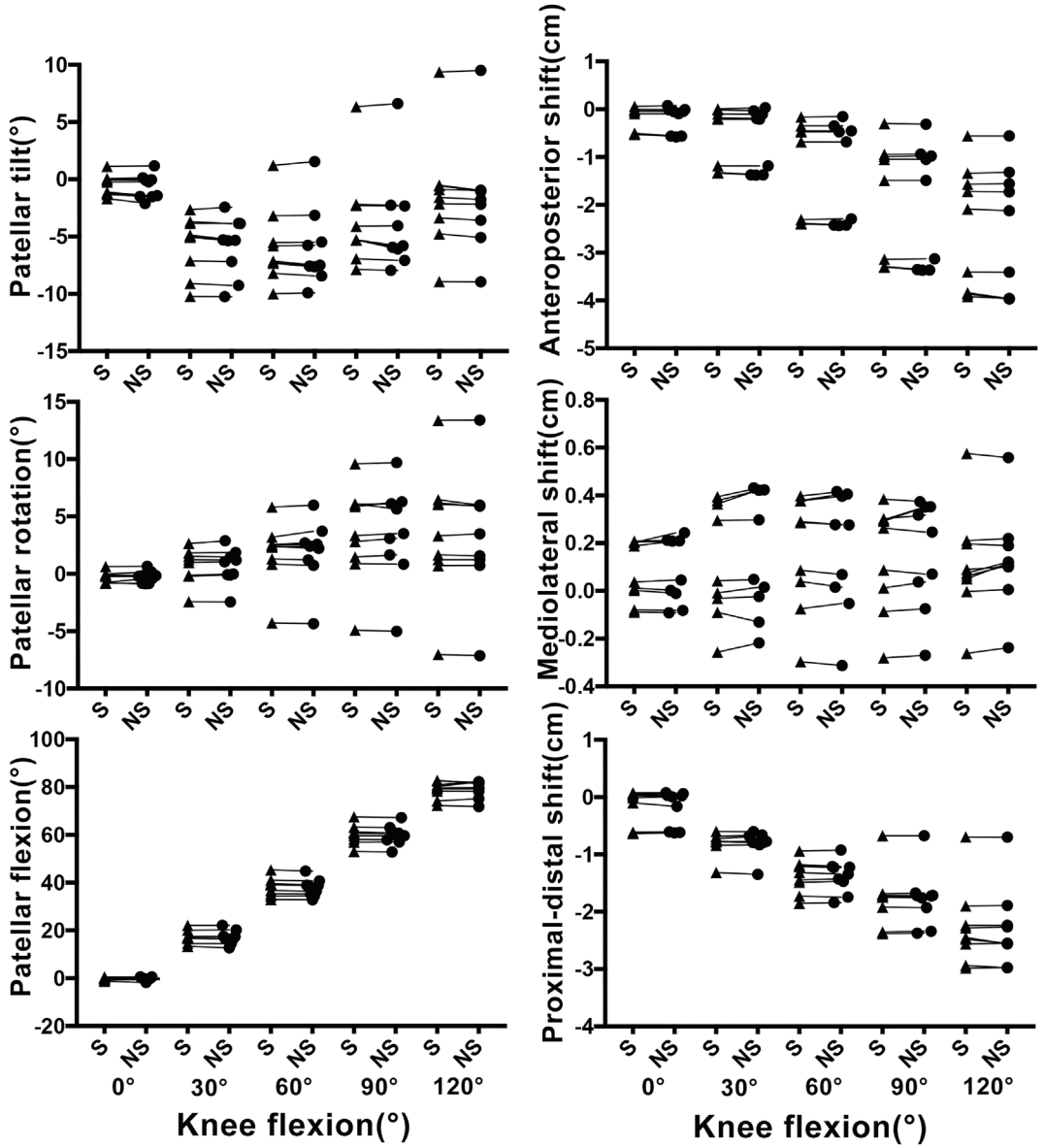

Fig. 5 Patellar kinematics of the knees with and without the inserted pressure sensor during knee flexion (▲: with the sensor; ●: without the sensor)

of knee flexion, the patella would shift medially. After 30° of knee flexion, the patella would progressively be shifting laterally and peaked at around 1.1 ± 0.7 mm at 90° of knee flexion. This was followed by a decreased lateral translation at the end of knee flexion.

Reliability of Kinematic Measurement Method

The results of the ICCs and MDDs for three motions are shown in Table 1. The intra-rater reliability of motions showed excellent correlation coefficients, ranging from 0.924 to 1. From Table 1, we found that the calculated MDDs for flexion, tilting and flexion were 0.35, 0.20, and 0.91°, respectively. The calculated MDDs for anteroposterior, proximal-distal, and medial-lateral translational were 0.25, 0.04, and 0.6 mm, respectively.

PFJ Kinematics with and without the Placement of the Pressure Sensor

The knees with the inserted pressure sensor showed similar patellar kinematic movement patterns as those without the pressure sensor (Fig. 5). No significant differences in PFJ kinematics were found between the two conditions during knee flexion at 0°, 30°, 60°, 90°, and 120° ($P > 0.05$).

PFJ Contact Areas and Pressure

A Representative Curve of the Contact Pressure in the PFJ during Knee Flexion

In a representative ACL-intact knee, the medial patellar facet showed a steady peak contact pressure during knee flexion. The medial patellar facet showed a range of 0.2 MPa (0.4 to 0.6 MPa) on the change of peak contact pressure during knee flexion, which was much smaller than MDDs of peak contact pressure when calculated on the medial patellar facet (0.54 MPa). Such that, this indicates no significant or detectable changes on this parameter during knee flexion. The lateral patellar facet demonstrated a progressively decreasing peak contact pressure, once the patella engaged the trochlear groove. At the initial flexion, the lateral patellar facet showed the highest peak contact pressure at 1.2 MPa. On the other hand, the peak contact pressure was found to decrease distinctively to 0.53 MPa when around 80° of knee flexion. When the patella began to leave the trochlear groove, the peak contact pressure would progressively increase. The lateral patellar facet showed a range of 0.7 MPa (0.5 to 1.2 MPa) on the change of peak contact pressure during knee flexion, which was larger than MDDs of peak contact pressure calculated on the lateral patellar facet (0.39 MPa). Importantly, the change of this parameter was found to be significant and detectable during knee flexion.

The exact mean/peak contact pressure and contact area of the PFJ in both and medial and lateral facet was shown in Fig. 6. No statistical differences of mean contact pressure were found between the medial and lateral PFJ compartment during the whole flexion. Regarding the peak contact pressure, lateral PFJ compartment demonstrated averagely

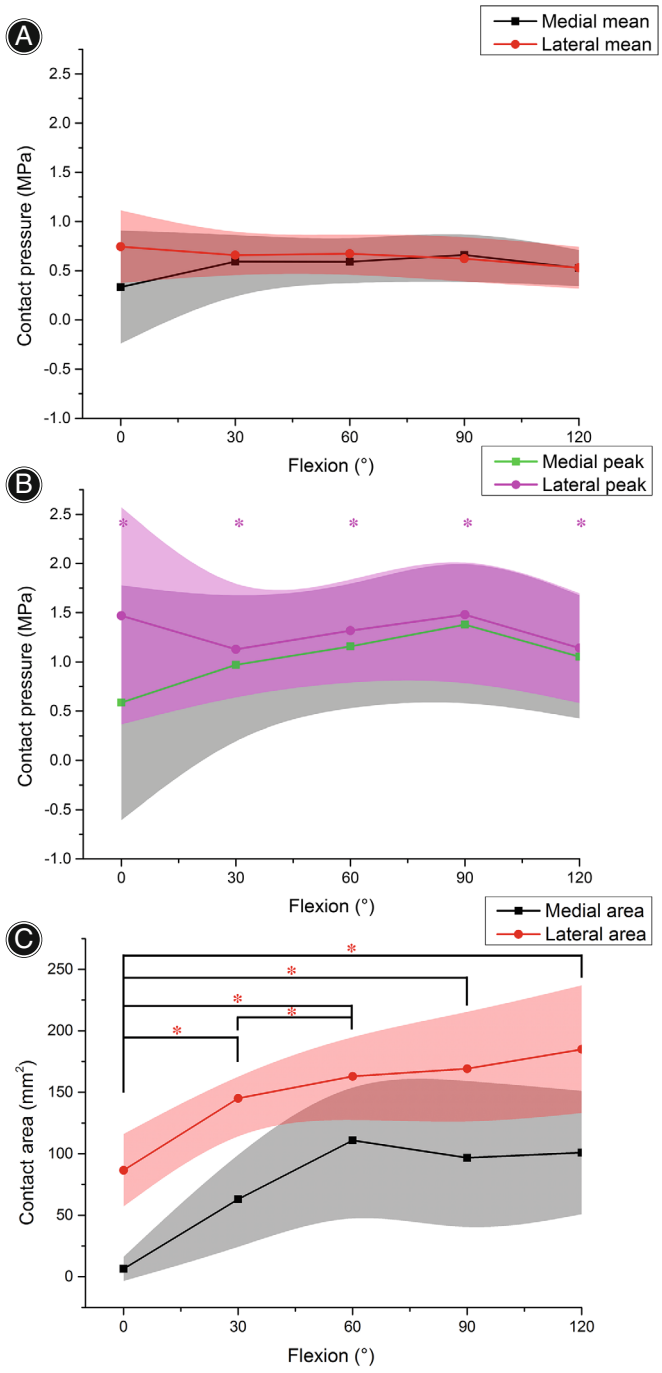

Fig. 6 Comparison of mean contact pressure, peak contact pressure and contact area in medial and lateral PFJ compartment during knee flexion. *$P < 0.05$

0.278 MPa (SD = 0.3) higher than those in medial compartment during the whole flexion procedure. Similarly, lateral PFJ compartment showed averagely 74.156 mm^2 larger than that located in medial PFJ compartment. At initial position, the PFJ compartment has statistically smaller contact area

TABLE 2 Intra-rater reliability (intra-class correlation) of contact mechanics in the PFJ

ICCs	At specific flexion angles					Overall	MDDs[a]
	0°	30°	60°	90°	120°		
Medial pressure	0.983	0.974	0.934	0.998	0.921	0.954	0.19
Lateral pressure	0.962	0.841	0.913	0.995	0.924	0.931	0.18
Medial peak	0.986	0.997	0.998	0.993	0.767	0.949	0.54
Lateral peak	0.918	0.965	0.996	0.947	0.757	0.937	0.39
Medial area	0.997	0.876	0.996	0.997	0.994	0.963	17.92
Lateral area	0.961	0.999	0.994	0.971	0.794	0.937	19.54

Abbreviations: MDDs, Minimal detectable changes; Medial/Lateral peak, Medial/Lateral peak contact pressure.; [a]The unite is MPa for pressure and mm^2 for area.

than other flexion angles no matter in medial or lateral compartment ($P < 0.05$). The effect of knee flexion had an impact on the specific compartment (interaction effect) when the outcome is mean contact pressure; however, no impact was found when the outcome is peak contact pressure or contact area.

For reproducibility, the ICCs and MDDs for the peak and mean contact pressure and contact area are shown in Table 2. All ICC values are over 0.75, indicating the protocol has good reliability. The calculated MDDs for mean contact pressure is 0.19 MPa and 0.54 MPa for peak contact pressure. The calculated MDDs for contact area is 19.54 mm^2.

Justification for Sensor Placement: Comparison of Referenced marks' Positions

A representative plot including the medial and lateral PFJ compartment is shown as Fig. 7 (Knee 6). A representative plot demonstrating that there were no positional alterations to the reference marks created on the sensor by the pins at different flexion angles during the knee flexion procedure is shown as Fig. 8. This figure indicates that there was no relative movement between the bone and the pressure sensor during knee flexion.

Discussion

The present study revealed several important findings. First, the remarkable reliability of the simultaneous kinematic and contact mechanics measurement protocol was confirmed, which demonstrated the reliability of our novel optical tracking system protocol for *in-vitro* PFJ kinematic and contact mechanical measurement. Second, no significant kinematic differences in the cadaveric knees were found before and after the insertion of the pressure sensor into the PFJ.

PFJ Kinematics and Contact Mechanics Measurement Methodology

In vitro biomechanical studies contain important assessments of the knee structure and function.[23] Many protocols have been used to measure *in vitro* kinematic data in cadaveric studies, including the model-based image-matching (MBIM) motion analysis technique from calibrated video sequences,[24] optoelectronic acquisition systems,[4] the fluoroscopy-based method,[25] and Roentgen stereophotogrammetric analysis (RSA).[25] The kinematic data derived from the bone-pin-marker-based protocol was considered to be the "gold standard" of measurement due to its high accuracy and reliability.[26] Optical tracking systems have been used in the measurement of PFJ kinematics in *in vitro* studies.[3,27] The algorithm applied in the current study was developed based on our previously-validated *in vivo* studies using the same apparatus.[28–30] The optical system enables researchers to simultaneously and synchronously collect real-time PFJ and TFJ kinematics and biomechanical data from the TekScan system, which is very beneficial in investigations of the association between the PFJ and TFJ. Some researchers found positive correlations between internal–external tibial rotation and lateral TFJ contact pressures in anterolateral tenodesis.[31] However, no previous researchers have sought to simultaneously quantify the PFJ kinematics and contact mechanics in cadaveric knees. This finding demonstrates the need to explore the potential relationship between the alterations of PFJ contact mechanics and TFJ kinematics in intact knees and injured knees with PFJ disorders.

Reliability and Accuracy Assessment for the PFJ Kinematics and Contact Mechanics

To examine the test–retest reliability of the patella's six DOF, ICCs were analyzed in the current study, and the results showed excellent correlation coefficients, especially for patellar flexion/extension and proximal/distal translation (ICC ≥0.999). The results obtained in the current study are consistent with those in previous *in vitro* studies in which the same coordinate system was used.[4] The low MDDs value of rotational freedom (less than 0.91°) and translational freedom (less than 0.6 mm) enabled the researchers to detect minimal differences at a high sensitivity level and interpret the changes accurately and confidently. Because the bone-pin-marker-based protocol has been regarded as the golden standard of kinematic measurement, investigating its validity was

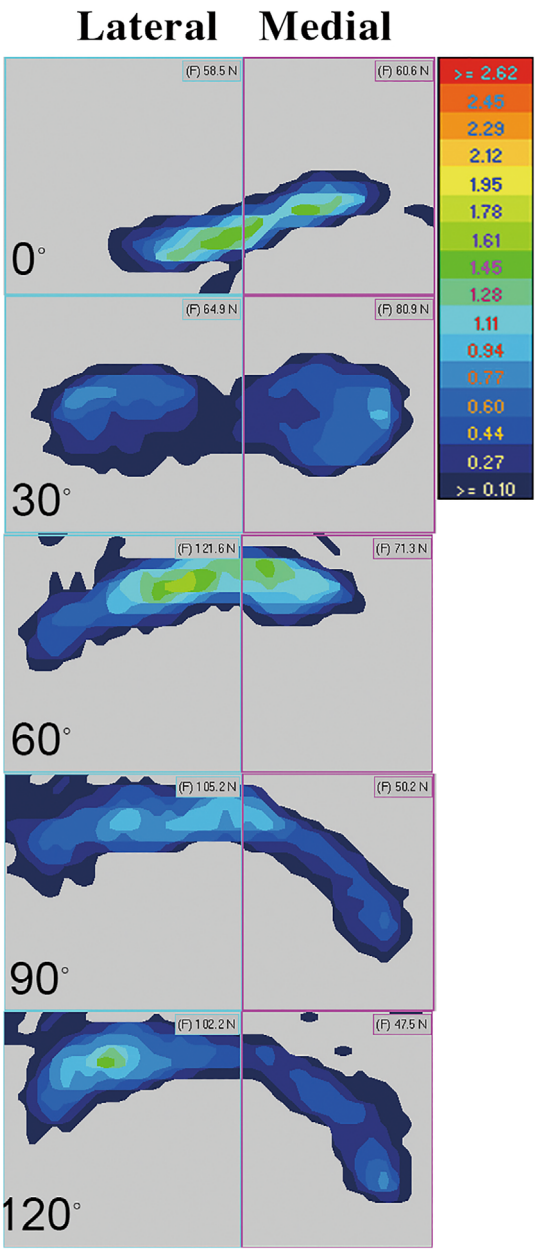

Fig. 7 Representative contact mapping of the patellofemoral joint during knee flexion. Medial, medial PFJ compartment; Lateral, lateral PFJ compartment

not necessary. Some researchers have reported the accuracy of rotational parameters reported to be within 0.03° and the accuracy of translational parameters to be within 0.03 mm.[27]

Specific Performances of PFJ Kinematics and Contact Mechanics during Knee Flexion

The current study showed medial tilting of the patella throughout the whole range of knee flexion. The results differ from a previous study in which lateral patellar tilting was shown.[4] This is likely due to the limited loads (10 Newton) being applied to the patella in the direction of the femur's anatomical axis in this previous study. These discrepancies indicated that the weight setting has a significant effect on patellar kinematics. For PFJ medial–lateral rotations, the patella consistently showed increasing lateral rotation in the current study. The rotations differ from those reported in previous studies.[4,32,33] Progressive lateral patellar translation, as shown in the current study, has also been reported in other studies. The patella gradually translated laterally up to a mean value of 1.7 mm during knee flexion. However, Philippot *et al.* reported a reverse movement pattern with a similar shift value (3.3 mm). This inconsistency demonstrated the significant effect of quadriceps muscle loading on the patellar tracking. Philippot *et al.*, applied a load of 10 N to the quadriceps tendon with a collinear anatomical axis of the femur, which is not a physiological muscle loading condition. For the application of MDDs, Stephen *et al.* reported that the transection of medial patellofemoral ligament (MPFL) significantly increased lateral patellar tilt (3.7 ± 8.9°) and lateral translation at full extension (3.3 ± 4.8 mm) compared to those of *in vivo* intact knees.[34] The MDDs of patellar rotation (0.9°) and translation (1 mm) using the optical tracking system in the current study enabled the researchers to identify significant clinical differences in these movement freedoms.

Effect of Sensor Placement and Placement Incision on the PFJ Contact Mechanics

Many previous researchers used I-Scan 5051 pressure sensors for PFJ contact mechanics measurement. In most cases, the I-Scan 5051 pressure sensor was able to cover the whole patellar area and was advantageous concerning the placement and securing of the sensor to the surface of the patella. The results of the current study indicate that this protocol is highly reliable for the measurement of PFJ contact mechanics. Although researchers have also used sensors to measure the contact mechanics in the PFJ, they utilized a medial or lateral incision for the placement of the sensor. This would affect the integrity of the medial or lateral patellofemoral ligament, respectively, leading to altered PFJ biomechanics.[10] To our knowledge, the current study is the first in which test–retest reliability was tested using the proposed incision and sensor. Besides the validation of the high reliability of medial peak pressure measurement in Knee 5 and lateral peak pressure measurement in Knee 7, excellent reliability was obtained in the remaining knees for different biomechanical parameters.

There were no significant differences in PFJ kinematics detected before and after the insertion of the pressure sensor, indicating that the PFJ biomechanical environment was not significantly affected by the placement of the thin sensor. In addition, to determine whether any technical errors were derived from the sensors themselves, we recorded the positions of the reference marks at every flexion angle mentioned above and compared the positions. The results showed that there were no positional alterations of the reference marks at

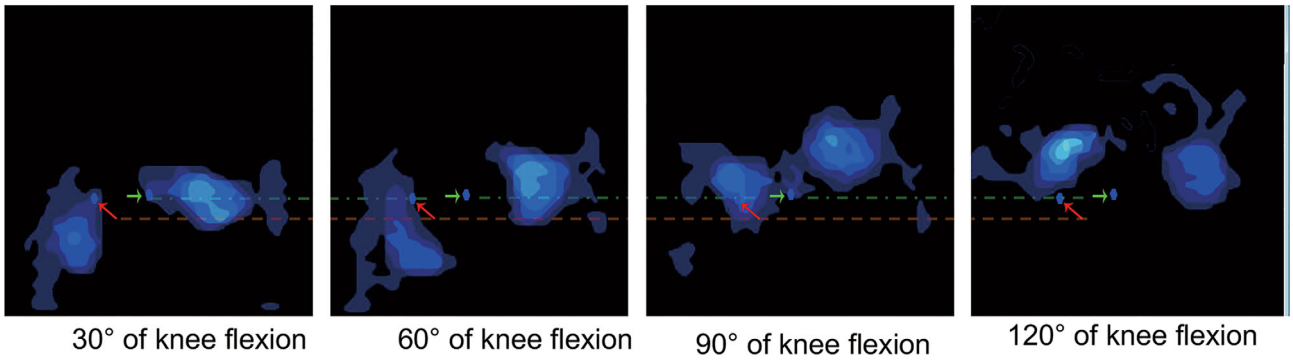

Fig. 8 A representative plot of contact mapping on the pressure sensor at different flexion angles during the knee flexion procedure. (Red arrow: reference mark on the medial patella; green arrow: reference mark on the lateral patella)

different flexion angles. This means that there was no relative movement between the sensor and the patella during knee flexion.

Limitations

There are some limitations in the current study. First, only quadriceps loading was applied in the anatomical directions. For simplification, hamstring loading was replaced by manual loading at the distal end of the tibia. Second, passive knee flexion (non-weight-bearing conditions) was performed in the cadaveric knees instead of squatting. Third, we did not investigate the effects of individual anatomical differences (such as sulcus angles and Insall–Salvati ratios) on the PFJ biomechanics. These limitations might have influenced our outcomes.

Conclusion

The low MDDs enabled the researchers to obtain an accurate interpretation of the kinematic and contact mechanics measurement using the experimental setting used in the present study. This technique for sensor placement can, therefore, provide accurate estimations of PFJ kinematics and biomechanical information. The setup in the present study enables researchers to simultaneously and synchronously collect real-time PFJ kinematics and tibiofemoral joint (TFJ) biomechanical kinematic data with high reliability.

Author Contribution

Wenhan Huang contributed to the conception or design of the current research; data collection, and manuscript drafting. Xiaolong Zeng contributed to drafting the article. Gene Chi-Wai Man contributed to drafting the article. Yang Liu contributed to the data collection and manuscript drafting, and Yu Zhang contributed to the conception or design of the current research

Acknowledgments

The authors thank the staff at the operation theater and Orthopaedics Learning Center at the Prince of Wales Hospital for providing the surgical instruments and technical assistance.

Supporting Information

Additional Supporting Information may be found in the online version of this article on the publisher's web-site:

Appendix S1: Supporting information

References

1. Loudon JK. Biomechanics and Pathomechanics of the patellofemoral joint. Int J Sports Phys Ther. 2016;11(6):820–30.
2. Rood A, Hannink G, Lenting A, Groenen K, Koëter S, Verdonschot N, et al. Patellofemoral pressure changes after static and dynamic medial patellofemoral ligament reconstructions. Am J Sports Med. 2015;43(10):2538–44.
3. Stephen JM, Kader D, Lumpaopong P, Deehan DJ, Amis AA. Sectioning the medial patellofemoral ligament alters patellofemoral joint kinematics and contact mechanics. J Orthop Res. 2013;31(9):1423–9.
4. Philippot R, Chouteau J, Testa R, Moyen B. In vitro analysis of patellar kinematics: validation of an opto-electronic cinematic analysis protocol. Knee Surg Sports Traumatol Arthrosc. 2010;18(2):161–6.
5. Farahmand F, Tahmasbi M, Amis A. Lateral force–displacement behaviour of the human patella and its variation with knee flexion—a biomechanical study in vitro. J Biomech. 1998;31(12):1147–52.
6. Koh TJ, Grabiner MD, De Swart RJ. In vivo tracking of the human patella. J Biomech. 1992;25(6):637–43.
7. Brossmann J, Muhle C, Schröder C, Melchert UH, Büll CC, Spielmann RP, et al. Patellar tracking patterns during active and passive knee extension: evaluation with motion-triggered cine MR imaging. Radiology. 1993;187(1):205–12.
8. Hsieh Y-F, Draganich LF, Ho SH, Reider B. The effects of removal and reconstruction of the anterior cruciate ligament on the contact characteristics of the patellofemoral joint. Am J Sports Med. 2002;30(1):121–7.
9. Chan K et al. Alteration of patellofemoral contact during healing of canine patellar tendon after removal of its central third. J Biomech. 2000;33(11):1441–51.
10. Van Haver A et al. Patellofemoral contact during simulated weight bearing squat movement: a cadaveric study. XII Mediterranean Conference on Medical and Biological Engineering and Computing 2010. New York: Springer; 2010.
11. Ostermeier S, Holst M, Hurschler C, Windhagen H, Stukenborg-Colsman C. Dynamic measurement of patellofemoral kinematics and contact pressure after lateral retinacular release: an in vitro study. Knee Surg Sports Traumatol Arthrosc. 2007;15(5):547–54.
12. Stephen JM, Kaider D, Lumpaopong P, Deehan DJ, Amis AA. The effect of femoral tunnel position and graft tension on patellar contact mechanics and

kinematics after medial patellofemoral ligament reconstruction. Am J Sports Med. 2014;42(2):364–72.
13. Beck P, Brown NAT, Greis PE, Burks RT. Patellofemoral contact pressures and lateral patellar translation after medial patellofemoral ligament reconstruction. Am J Sports Med. 2007;35(9):1557–63.
14. Mikula JD, Slette EL, Dahl KD, Montgomery SR, Dornan GJ, O'Brien L, et al. Intraarticular arthrofibrosis of the knee alters patellofemoral contact biomechanics. J Exp Orthop. 2017;4(1):40.
15. Stephen JM, Kittl C, Williams A, Zaffagnini S, Marcheggiani Muccioli GM, Fink C, et al. Effect of medial patellofemoral ligament reconstruction method on patellofemoral contact pressures and kinematics. Am J Sports Med. 2016;44(5):1186–94.
16. Kalichman L, Zhang Y, Niu J, Goggins J, Gale D, Felson DT, et al. The association between patellar alignment and patellofemoral joint osteoarthritis features an MRI study. Rheumatology. 2007;46(8):1303–8.
17. Sakai N, Luo ZP, Rand JA, An KN. The influence of weakness in the vastus medialis oblique muscle on the patellofemoral joint: an in vitro biomechanical study. Clin Biomech. 2000;15(5):335–9.
18. Amis AA, Senavongse W, Bull AM. Patellofemoral kinematics during knee flexion-extension: an in vitro study. J Orthop Res. 2006;24(12):2201–11.
19. Shalhoub S, Maletsky LP. Variation in patellofemoral kinematics due to changes in quadriceps loading configuration during in vitro testing. J Biomech. 2014;47(1):130–6.
20. Farahmand F, Sejiavongse W, Amis AA. Quantitative study of the quadriceps muscles and trochlear groove geometry related to instability of the patellofemoral joint. J Orthop Res. 1998;16(1):136–43.
21. Grood ES, Suntay WJ. A joint coordinate system for the clinical description of three-dimensional motions: application to the knee. J Biomech Eng. 1983;105(2):136–44.
22. Fleiss JL. Reliability of measurement. The Design and Analysis of Clinical Experiments. New York: Willey; 1986. p. 1–32.
23. Hatze H. Letter: the meaning of the term "biomechanics". J Biomech. 1974;7(2):189–90.
24. Mok K-M, Fong DTP, Krosshaug T, Hung ASL, Yung PSH, Chan KM. An ankle joint model-based image-matching motion analysis technique. Gait Posture. 2011;34(1):71–5.
25. Tang T et al. Fluoroscopy-based method accurately assesses three-dimensional kinematics of the patellofemoral joint. Orthopaedic Proceedings. London, UK: British Editorial Society of Bone and Joint Surgery; 2008.
26. Benoit DL, Ramsey DK, Lamontagne M, Xu L, Wretenberg P, Renström P. Effect of skin movement artifact on knee kinematics during gait and cutting motions measured in vivo. Gait Posture. 2006;24(2):152–64.
27. Iranpour F, Merican AM, Baena FRY, Cobb JP, Amis AA. Patellofemoral joint kinematics: the circular path of the patella around the trochlear axis. J Orthop Res. 2010;28(5):589–94.
28. Huang W, Lin Z, Zeng X, Ma L, Chen L, Xia H, et al. Kinematic characteristics of an osteotomy of the proximal aspect of the fibula during walking: a case report. JBJS Case Connect. 2017;7(3):e43.
29. Zhang Y, Huang W, Yao Z, Ma L, Lin Z, Wang S, et al. Anterior cruciate ligament injuries alter the kinematics of knees with or without meniscal deficiency. Am J Sports Med. 2016;44(12):3132–9.
30. Zhang Y, Yao Z, Wang S, Huang W, Ma L, Huang H, et al. Motion analysis of Chinese normal knees during gait based on a novel portable system. Gait Posture. 2015;41(3):763–8.
31. Inderhaug E, Stephen JM, el-Daou H, Williams A, Amis AA. The effects of anterolateral tenodesis on tibiofemoral contact pressures and kinematics. Am J Sports Med. 2017;45(13):3081–8.
32. Philippot R, Boyer B, Testa R, Farizon F, Moyen B. Study of patellar kinematics after reconstruction of the medial patellofemoral ligament. Clin Biomech. 2012;27(1):22–6.
33. Ramappa AJ, Apreleva M, Harrold FR, Fitzgibbons PG, Wilson DR, Gill TJ. The effects of medialization and anteromedialization of the tibial tubercle on patellofemoral mechanics and kinematics. Am J Sports Med. 2006;34(5):749–56.
34. Stephen JM, Dodds AL, Lumpaopong P, Kader D, Williams A, Amis AA. The ability of medial patellofemoral ligament reconstruction to correct patellar kinematics and contact mechanics in the presence of a lateralized tibial tubercle. Am J Sports Med. 2015;43(9):2198–207.